

Optimal Design of a Cylindrical Voice Coil Actuator Based on Non-Dominated Sorting Genetic Algorithm-II

Suorena Saeedi

Dept. of Mechanical Engineering
University of Tehran
Tehran, Iran
suorena.saeedi@ut.ac.ir

Ali Sadighi

Dept. of Mechanical Engineering
University of Tehran
Tehran, Iran
asadighi@ut.ac.ir

Masoud Shariat Panahi

Dept. of Mechanical Engineering
University of Tehran
Tehran, Iran
mshariatp@ut.ac.ir

Abstract— Cylindrical Voice Coil Actuators (CVCA) are easy to launch, control, and maintain. Therefore, they are widely used in various industries, especially in the field of precision motion applications. During the design stage, in addition to certain performance requirements such as force and stroke, space limitations should also be taken into account. Solving such a problem is a cumbersome task when many variables, constraints, and conflicting objectives are involved. In this paper, we formulate a multi-objective optimization problem to minimize cylindrical voice coil actuator dimensions through the governing electromagnetic equations of the actuator. Using the Non-Dominated Sorting Genetic Algorithm-II (NSGA-II), the optimization problem is solved for the dimensions of the actuator given the specified performance metrics. The design obtained through optimization is then validated by calculating magnetic flux distribution and electromagnetic force using Finite-Element Analysis (FEA) and comparing them against the specification.

Keywords—Voice Coil Actuators, multi-objective optimization, Non-Dominated Sorting Genetic Algorithm-II, Finite element analysis

I. INTRODUCTION

Voice coil actuators are linear actuators with limited motion course. The voice coil actuator structure (VCA) consists of a permanent magnet and a coil. The magnetic circuit in the actuator is designed to direct the magnetic flux toward the air gap where the current-carrying coil will be forced to move according to Lorentz force law.

The voice coil actuators have a wide range of applications due to their advantages over other linear actuators. These actuators have been popular for their simple structure, fast response, high acceleration, high-frequency actuation, and high efficiency in converting electrical to mechanical energy [1], [2]. In addition, these actuators are widely used in precision motion applications because they are free from mechanical hysteresis, force ripple, and backlash, due to their non-contact and continuous operation [3]. These advantages have made voice coil actuators to be used in many applications such as fuel injection systems [4], computer disk drives, audio loudspeakers [1], air bearings [3], needle-free jet injection [5], and so on. In many of these applications, the space occupied by the actuator is very important, and optimizing the dimensions of the actuator can be critical.

Although the voice coil actuators have a simple structure, their optimal design is a significant problem. However, in the optimal design of VCAs, depending on their application, there can be various objectives. In [6], the optimal design of an optical disk drive VCA is done by applying design of

experiments (DOE) and response surface method (RSM) techniques to optimize output power and compactness. In [7], the optimal design of a type of VCA is reached using genetic algorithm (GA). The cost function is defined in such a way to maximize actuator sensitivity through providing maximum uniform electromagnetic force with the lowest power consumption and within the smallest size. Optimal design of a VCA for optical image stabilization is introduced in [8] based on GA. Minimization of the geometric dimensions of a type of VCA as a multi-objective optimization problem is defined in [9], which is solved by the output space mapping (OSM) method.

There are different shapes of VCAs, but CVCA is one of the most popular types of VCAs and it has numerous applications. So, the optimal design of CVCA has drawn plenty of attention from diverse research fields. [10] present a combination method of the improved sequential optimization method (SOM) and dimension reduction optimization method (DROM) to minimize the total mass of CVCA. Also in [5], the CVCA mass of a needle-free jet injection system is optimized with the sequential quadratic programming (SQP) algorithm. In [11], the geometric dimensions of a CVCA are minimized by means of a single-objective optimization method, in which the objective function is defined as a combination of geometric dimensions, and then by the Space Mapping (SM) method, this objective function is minimized by considering constraints. [3] obtains the optimal design for a CVCA by solving a multi-objective optimization problem to maximize acceleration and minimize heat dissipation. In [12], optimal design to minimize the response time of a CVCA, that is used in fast-switching valve, achieved. And in [4], main structural parameters of a CVCA that used in an injection fuel system is optimized by the magnetic equivalent circuit (MEC) method to maximize the flow rate of the injector.

In this paper, we formulate the design of a CVCA with certain specifications as a multi-objective optimization problem which aims to minimize the overall actuator size. In section II, the magnetic circuit analysis and modeling of the actuator are performed. Section III describes the optimization problem. In section IV, we use finite-element analysis to verify the optimization results.

II. MAGNETIC CIRCUIT

The CVCA consists of a cylindrical iron core with a permanent magnet in the center and a cylindrical coil in which the coil is placed inside the iron core in such a way that the current of the coil is perpendicular to the flux lines.

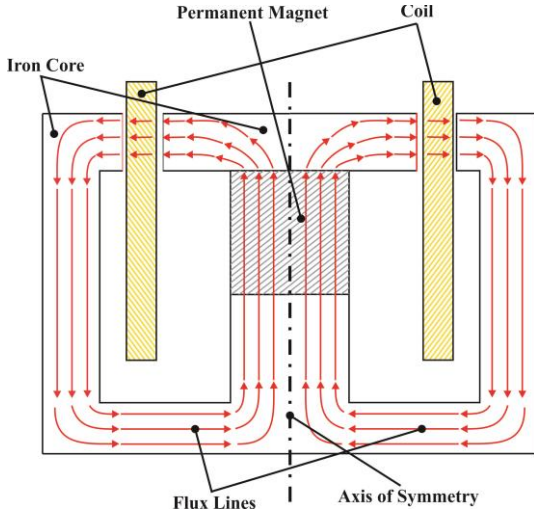


Fig. 1. Overview of the CVCA.

As shown in Fig.1, in the CVCA the flux lines are perpendicular to the current of the coil, so according to the Lorentz force law:

$$F = i_w l_w B_g \quad (1)$$

Where F represents the Lorentz force in the direction of the axis of symmetry, i_w represents the current of the coil, l_w represents the length of the coil wire through which the flux lines pass, and B_g is the magnitude of the magnetic flux density in the air gap.

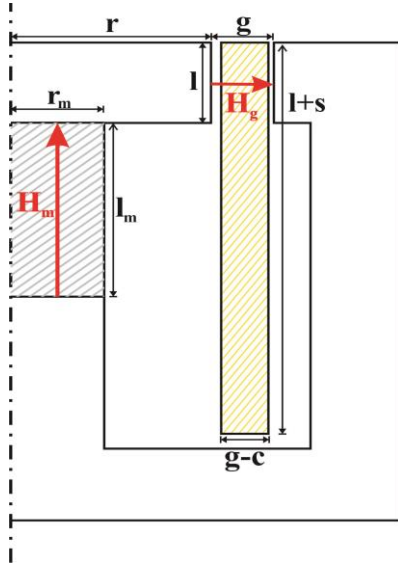


Fig. 2. Design parameters of CVCA, and magnetic field vector inside the permanent magnet and air gap.

Fig. 2 shows the geometric parameters that have the greatest impact on CVCA performance, which we consider as design parameters and ignore the slight influence of other geometric parameters. Also, according to Fig. 2, the length of the coil wire through which the flux lines pass can be estimated as follows:

$$l_w = 2\pi N_w (r + g/2) \quad (2)$$

Where N_w represent number of the coil wire through which the flux lines pass, r represent internal radius of the iron core, and g is the air gap. Also, by considering the concept of the

current density (J), current of the coil can be calculated as follows:

$$i_w = l(g - c)J/N_w \quad (3)$$

Where c is the clearance, so according to equations 1, 2, and 3, the equation of Lorentz force can be written as follows:

$$F = 2\pi(r + g/2)l(g - c)JB_g \quad (4)$$

Also according to the Ampere's law:

$$\oint H \cdot dl = 0 \rightarrow H_m = -\frac{g}{l_m \mu_0} B_g \quad (5)$$

Where H_m represents the magnetic field of the permanent magnet, l_m represents length of the permanent magnet, and μ_0 is the air permeability and its value is $4\pi \times 10^{-7}$ H/M. Also according to the Gauss's law:

$$\oint B \cdot da = 0 \rightarrow B_m = \frac{2rl}{r_m^2} B_g \quad (6)$$

Where B_m represents the magnitude of the magnetic flux density in the permanent magnet, and r_m is radius of the permanent magnet.

The following equation can also be used to estimate the equivalent resistance of the coil:

$$R = \rho L_w / A \quad (7)$$

Where R represents equivalent resistance of the coil, ρ represents the resistivity, and assuming that the coil wire is made of copper, its value is equal to 1.68×10^{-8} $\Omega \cdot m$, L_w represents whole length of the coil wire, and A is the cross-sectional area of the wire, which can be estimated as follows:

$$A = (g - c)(l + s) / N \quad (8)$$

Where s represents actuator stroke length, and N is number of the coil wire, L_w can also be estimated as follows:

$$L_w = 2\pi N (r + g/2) \quad (9)$$

So, according to (7), (8), and (9) equivalent resistance of the coil can be written as follows:

$$R = 2\pi\rho N^2 \frac{(r + g/2)}{(g - c)(l + s)} \quad (10)$$

And the coil current calculated in (3) can be written in another way:

$$i_w = (l + s)(g - c)J/N \quad (11)$$

Also, according to (10), and (11) the supply voltage of the coil can be calculated as follows:

$$V = i_w R = 2\pi\rho N J (r + g/2) \quad (12)$$

Finally, according to (11), and (12) we can calculate the electrical power of the actuator as follows:

$$P = i_w V = 2\pi\rho J^2 (r + g/2) (g - d)(l + s) \quad (13)$$

III. OPTIMIZATION

In the previous section, the CVCA governing electromagnetic equations were obtained. In this section, we try to define a multi-objective optimization problem through these equations to achieve the optimal design of the actuator.

The first objective of this optimization is to minimize internal radius of the iron core (r) because reducing r not only reduces the mass and space occupied by the actuator but also reduces the internal radius of the coil, which in turn reduces the mass of the rotor. According to (4) and (5), internal radius of the iron core can be calculated according to design parameters:

$$r = \frac{B_g F + \pi H_m l_m \mu_0 (-H_m l_m \mu_0 - c) l J}{2\pi (-H_m l_m \mu_0 - c) l J B_g} \quad (14)$$

The second objective is to minimize the air gap (g), which directly reduces coil mass and increases actuator bandwidth. Based on (5), the air gap can be written based on design parameters:

$$g = -\frac{H_m l_m \mu_0}{B_g} \quad (15)$$

The third and final objective of optimization is to minimize radius of the permanent magnet (r_m) because it reduces the cost of manufacturing and assembling the CVCA. And according to (4), (5), and (6) radius of the permanent magnet can be calculated according to design parameters:

$$r_m = \sqrt{\frac{B_g F + \pi H_m l_m \mu_0 l J (-H_m l_m \mu_0 - c)}{\pi B_m J (-H_m l_m \mu_0 - c)}} \quad (16)$$

It is assumed that Grade 42 neodymium-iron-boron (NdFeB) Magnet is used in the design of this actuator. There is also a tendency for the magnet to work in a zone where the magnet energy is maximum.

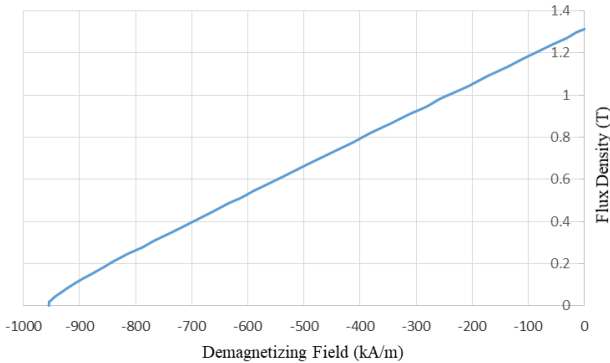


Fig. 3. B-H curve of grade 42 neodymium-iron-boron magnet at 20°C.

The energy of the magnet (E_m) is the product of the magnetic flux density and the magnetic field of the magnet, and assuming that the working temperature of the magnet is 20°C, according to Fig. 3, the working point at which the magnet has the most energy is as follows:

$$\frac{dE_m}{dH_m} = 0 \rightarrow \begin{cases} H_m = -477.5 \text{ kA/m} \\ B_m = 0.65 \text{ T} \end{cases}$$

Also, according to the application of the CVCA, its force (F) is considered equal to 15N and its stroke (s) is equal to 65mm. And due to the manufacturing constraints, the value of the clearance (c) is considered equal to 2mm.

Another constraint on this problem is that the electrical power of the actuator should not exceed 40w:

$$P \leq P_{max} = 40w$$

Besides, according to the actuator's geometry, we know that the radius of the permanent magnet (r_m) should not be less than zero and not greater than the internal radius of the iron core (r).

$$0 < r_m \leq r$$

And as a final constraint, we know that the thickness of the coil ($g - c$) must be greater than zero.

$$g - c > 0$$

Therefore, the optimization model is defined as follows:

$$\text{Min: } \begin{cases} r: \text{ internal radius of the iron core} \\ g: \text{ air gap} \\ r_m: \text{ radius of the permanent magnet} \end{cases}$$

$$\text{s. t. } \begin{cases} g_1: H_m = -477.5 \text{ kA/m} \\ g_2: B_m = 0.65 \text{ T} \\ g_3: F = 15 \text{ N} \\ g_4: s = 65 \text{ mm} \\ g_5: c = 2 \text{ mm} \\ g_6: P \leq P_{max} = 40 \text{ W} \\ g_7: 0 < r_m \leq r \\ g_8: g - c > 0 \end{cases}$$

TABLE I. The Design parameters and ranges.

Par	Definition	Unit	Min	Max
B_g	magnitude of the magnetic flux density in the air gap	T	0	2
J	current density in the coil	A/mm ²	0	6.5
l_m	length of the permanent magnet	mm	0	900
l	The length required to cross the magnetic flux	mm	0	90

TABLE I. shows the design parameters and the acceptable range of their changes. In the next step, this multi-objective optimization problem is solved using the NSGA-II, and to do so, the optimization toolbox of MATLAB 2018b is used.

TABLE II. Optimization parameters.

Parameter	Value
Initial population	1000
Crossover fraction	0.75
Function tolerance	10 ⁻⁵
Constraint tolerance	10 ⁻⁶

In the optimization toolbox, gamultiobj solver is considered to use the NSGA-II to solve the problem and after defining the mentioned multi-objective optimization problem, the optimization parameters are set as shown in Table II. Other settings are set to the default value and then the algorithm is run.

Finally, the algorithm converges after 1371 generations and Pareto optimal front can be seen in Fig. 4. Since it contains non-dominated points, each point can represent an optimal design. Finally, considering the manufacturing constraints and manufacturing and assembly costs, a point of Pareto optimal front has been selected as the final optimal design.

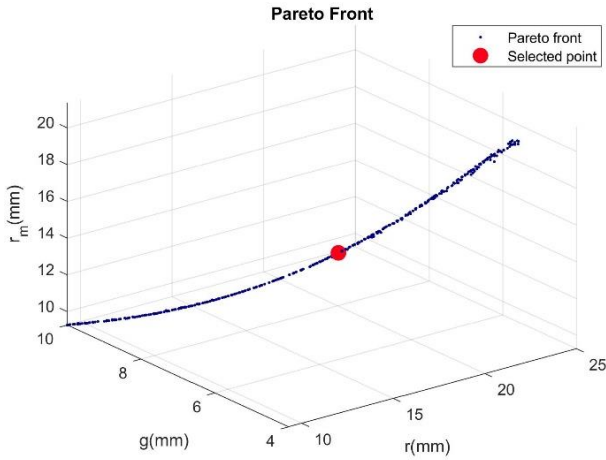


Fig. 4. Pareto optimal front and the point selected as the optimal design.

So, the optimal design acquired from the NSGA-II, which includes the objective functions and variables of the selected point from Pareto optimal front, can be seen in Table III.

TABLE III. Optimal design parameters of CVCA.

Par	Unit	Value
r	mm	15
g	mm	5
r_m	mm	15
J	A/mm ²	6
l_m	mm	60
l	mm	1

IV. FINITE ELEMENT ANALYSIS

In this section, according to the optimal design parameters obtained in the previous section, the CVCA is simulated and its performance is investigated. ANSYS Maxwell 16 is used to simulate the actuator's performance. In this simulation, the iron core is made of steel 1010, the coil is made of copper, and the permanent magnet is made of Grade 42 NdFeB. The coil is also mounted on an aluminum rotor so as not to affect the actuator's magnetic circuit.

Parameters x_1 , x_2 , and x_3 are geometrical parameters, and they have been selected based on experience so that electromagnetic saturation does not occur in the iron core. These parameters do not play a significant role in the actuator's performance and their size should be chosen so large that the saturation in the iron core does not occur. Therefore, their size depends to some extent on the iron core material. Fig. 5 indicates the value of these parameters and the

optimal design of the operator, which shows all the dimensions and the material of the various components of the CVCA and how they are assembled.

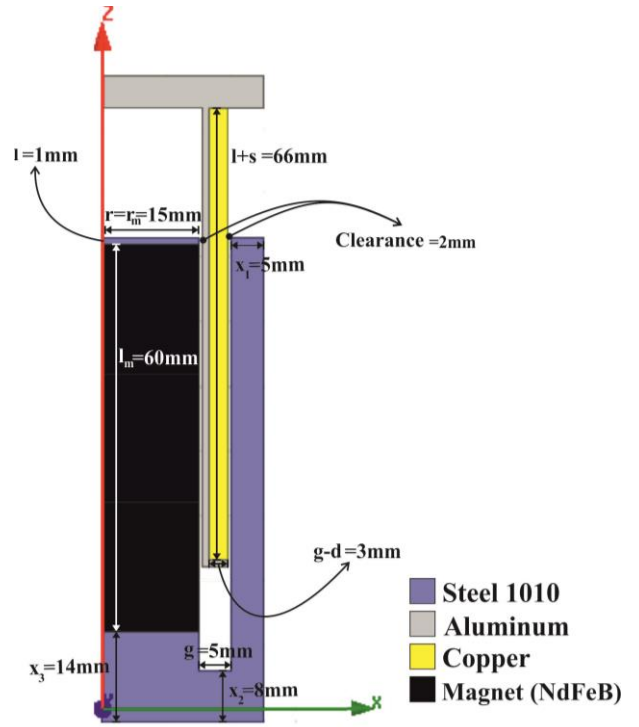


Fig. 5. Optimal design of the CVCA.

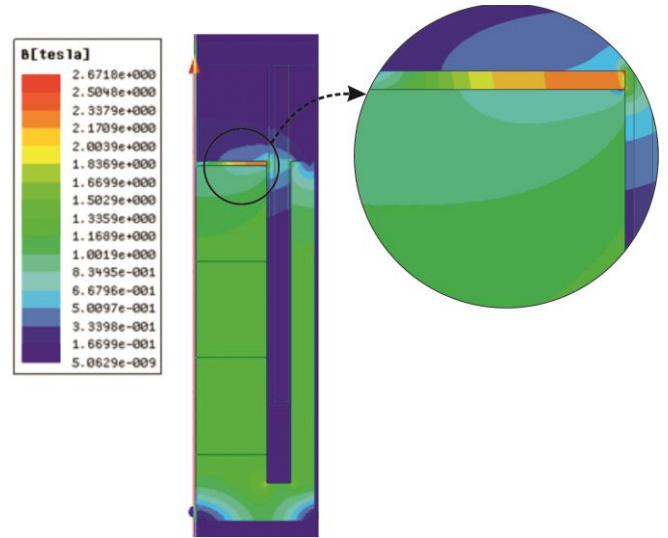


Fig. 6. The magnetic flux density of the designed CVCA.

Fig. 6 shows the magnetic flux density in different regions of the CVCA. As it is seen, the magnetic flux density is uniform in most areas of the iron core, and the magnetic capacity of the iron core is well used. Only in a small zone of the iron core at the top of the permanent magnet did the magnetic flux density exceed the allowable limit and electromagnetic saturation occurred. Although this small area does not greatly affect the actuator's performance, but to ensure that no saturation problem occur in any part of the iron core, and also because of the challenges that may arise in the manufacturing process due to the low thickness of this part, in the final design we increase the thickness of the area above the

permanent magnet (I) from 1mm that obtained from the optimization to 6mm.

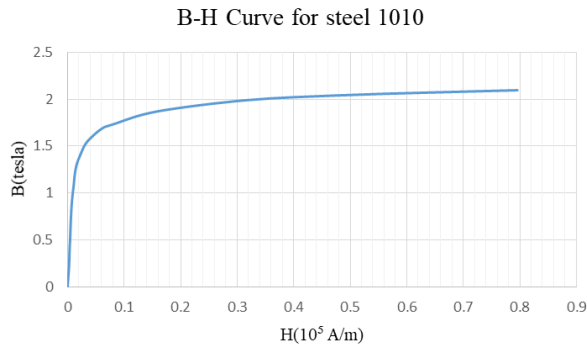


Fig. 7. Nonlinear magnetization curve for steel 1010.

Fig. 7 shows that the magnetization curve for steel 1010 has a linear behavior as long as the flux density is less than 1.5T, and enters the saturation zone for higher values. In Fig.6, it can be seen that in the part of the iron core located at the top of the permanent magnet, the flux density increases by more than 2T, and the electromagnetic saturation occurs in this area.

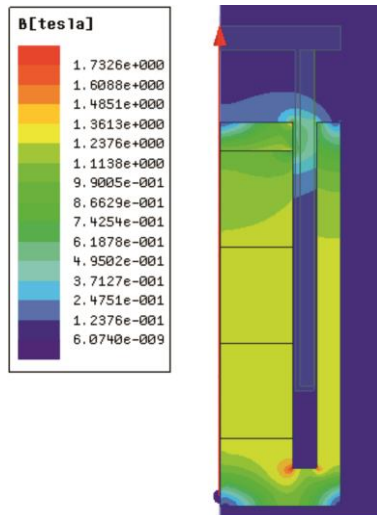


Fig. 8. The magnetic flux density from the final designed CVCA.

Fig. 8 shows that by increasing the thickness of the iron core in the upper region of the permanent magnet (I), the problem of electromagnetic saturation in the actuator is completely solved, although, this increases the height of the coil as well as the height of the actuator by 5 mm compared to the optimal design.

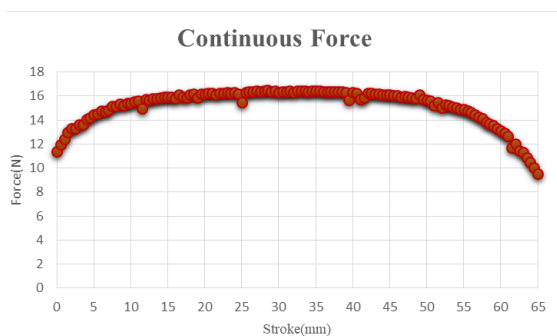


Fig. 9. The CVCA force along its stroke.

Fig. 9 shows the CVCA force obtained using FEA at 0.5mm intervals over the range of motion and assuming a coil current density of 6A/mm². It can be seen that the CVCA force is constant for most of the stroke length, and it is in the desired range. So, it can be said that the CVCA designed based on the optimization is able to generate the force considered in the design phase along the assumed stroke.

V. CONCLUSION

In this paper, the design of a CVCA based on the governing electromagnetic equations is defined as a multi-objective optimization problem to minimize some of the geometric dimensions of the actuator with a certain force and stroke. By minimizing these geometric dimensions, mass of the rotor, mass of the permanent magnet, and the manufacturing and assembly costs are minimized, and the actuator bandwidth is maximized. The problem of multi-objective optimization is solved with NSGA-II, and the optimal design of the CVCA is selected from the Pareto optimal front.

However, since material of the actuator's iron core and its nonlinear magnetization behavior were not considered, electromagnetic saturation was observed in the finite element analysis of the actuator. Finally this problem was solved with increasing the thickness of the iron core in the upper region of the permanent magnet and the final design obtained for the CVCA was able to satisfy force and stroke specifications.

REFERENCES

- [1] X. M. Feng, Z. J. Duan, Y. Fu, and A. L. Sun, "The Technology and Application of Voice Coil Actuator," *Int. Conf. Mech. Autom. Control Eng.*, pp. 892–895, 2011.
- [2] T. Stroehla, M. Dahlmann, T. Kellerer, T. Wagner, N. Wagner, and T. Sattel, "Ultra-fast moving coil actuator for power switches in medium-voltage grids," *Int. Conf. Power Electron. Mach. Drives*, vol. 2019, no. 17, pp. 4085–4089, 2019.
- [3] A. Okyay, M. B. Khamesee, and K. Erkorkmaz, "Design and Optimization of a Voice Coil Actuator for Precision Motion Applications," *IEEE Trans. Magn.*, vol. 51, no. 6, 2015.
- [4] H. Gao, F. Zhang, W. Zeng, T. Dong, and Z. Wang, "Design and Optimization of Injector Based on Voice Coil Motor," *SAE Int.*, 2017.
- [5] B. P. Ruddy, A. W. Dixon, R. Michael, J. Williams, and A. J. Taberner, "Optimization of Portable Electronically Controlled Needle-Free Jet Injection Systems," *IEEE/ASME Trans. MECHATRONICS*, vol. 22, no. 5, pp. 2013–2021, 2017.
- [6] D. Lee, K. Woo, N. Park, and Y. Park, "Design and Optimization of a Linear Actuator for Subminiature Optical Storage Devices," *IEEE Trans. Magn.*, vol. 41, no. 2, pp. 1055–1057, 2005.
- [7] C. Chiu, P. C. Chao, and D. Wu, "Optimal Design of Magnetically Actuated Optical Image Stabilizer Mechanism for Cameras in Mobile Phones via Genetic Algorithm," *IEEE Trans. Magn.*, vol. 43, no. 6, pp. 2582–2584, 2007.
- [8] M. Song *et al.*, "Design of a Voice-Coil Actuator for Optical Image Stabilization Based on Genetic

Algorithm,” *IEEE Trans. Magn.*, vol. 45, no. 10, pp. 4558–4561, 2009.

- [9] S. Vivier, D. Lemoine, and G. Friedrich, “Fast Optimization of a Linear Actuator by Space Mapping Using Unique Finite-Element Model,” *IEEE Trans. Ind. Appl.*, vol. 47, no. 5, pp. 2059–2065, 2011.
- [10] A. M. T. Corp, “Optimization Design of a Voice Coil Actuator Based on Improved SOM,” 2011.
- [11] L. Encica, J. Makarovic, E. A. Lomonova, and A. J. A. Vandenput, “Space Mapping Optimization of a Cylindrical Voice Coil Actuator,” *IEEE Trans. Ind. Appl.*, vol. 42, no. 6, pp. 1437–1444, 2006.
- [12] D. B. Roemer, M. M. Bech, P. Johansen, and H. C. Pedersen, “Optimum Design of a Moving Coil Actuator for Fast-Switching Valves in Digital Hydraulic Pumps and Motors,” *IEEE/ASME Trans. MECHATRONICS*, pp. 1–10, 2015.